

Energetics of large lattice strains: Application to silicon

Efthimios Kaxiras

Department of Physics and Division of Applied Sciences, Harvard University, Cambridge, Massachusetts 02138

L. L. Boyer

Complex Systems Theory Branch, Naval Research Laboratory, Washington, D.C. 20375

(Received 11 November 1993; revised manuscript received 25 January 1994)

We discuss the mathematical formalism of physically allowed lattice-invariant strains. When coupled with first-principles calculations of the energy as a function of strain, this approach becomes a powerful tool for understanding large lattice strains in solids. We also present an application of this tool to explore deformations of silicon, which predicts, to our knowledge, a previously unknown metastable structure. The physical properties of this structure are described and a method for obtaining it experimentally is explicitly provided.

I. INTRODUCTION

Structural transformations in solids play an important role in understanding their mechanical stability, strength, response to applied forces, resistance to heat, etc. In order to describe structural transformations from a theoretical point of view one must be able to calculate accurately several aspects of a solid's behavior, all of them related to the energetics of distortions from an equilibrium structure. There are many examples of first-principles quantum mechanical calculations of the energy of solids as a function of small variations in crystal structure, from which phonon modes and elastic constants can be determined. First-principles calculations comparing the energies of elements and compounds in widely differing, but locally stable structures are also common. On the other hand, there are relatively few examples of total energy calculations for crystal distortions large enough to transform *continuously* between two widely different structures. Such transformations necessarily involve large lattice strains (LLS), i.e., strains beyond the elastic limit. In this paper, we address this class of deformations, first by developing the proper formalism and then by applying it to a representative covalent solid, silicon.

The paper is organized as follows: Sec. II cites recent work involving LLS. Section III describes the formalism of LLS by defining physically-allowed lattice-invariant (PALI-) strain matrices and provides an example on the fcc lattice. Section IV discusses the application of PALI-strain transformations to silicon, the identification of a metastable phase and the structural and electronic properties of this phase. Section V provides an account of how this phase might be formed experimentally. Section VI concludes with some remarks on the usefulness of our approach.

II. BACKGROUND TO LARGE LATTICE STRAIN CALCULATIONS

Wills *et al.*¹ have recently pointed out a correlation between the shear modulus $c_{11}-c_{12}$, in fcc metals, and the

difference between the energy in the bcc and fcc structures. The correlation can be understood by noticing that the $c_{11}-c_{12}$ distortion begins along the path which transforms fcc to bcc, the so-called Bain strain. There exists yet another correlation, which becomes evident when one more dimension is added to the strain space explored by Wills *et al.* Specifically, Mehl and Boyer² showed that the lowest energy path for PALI strains in aluminum and iridium deviates from the Bain path in the region of the bcc structure, and has a barrier that correlates roughly with the melting temperature (T_m). This correlation has been noted in other materials as well,³ and could be the fundamental reason why trends in elastic constants generally correlate with trends in the melting temperature. In a parallel and independent development, Wang, Yip, Phillpot, and Wolf⁴ have recently proposed stability criteria for crystals, based on stress-strain relations at finite deformation.

Knowledge of the energetics associated with LLS may provide a key to understanding many complicated physical processes, which involve the nucleation, disintegration, and transformation of crystal lattices. Examples include solid-liquid transitions, martensitic transformations, amorphization (which can be induced by various methods, including mechanical stress), and mechanical properties outside the elastic region. In all these cases, large deformations akin to LLS are involved, possibly at various length scales. Developing a framework for calculating accurately LLS is crucial to the theoretical description of these phenomena.

The basic concept of PALI strains, that is, symmetric strain tensors which transform a lattice into itself, was developed only recently.^{5,6} PALI strains are significant in at least two respects:

- (i) they aid in identifying low energy domains in strain space; and
- (ii) they can, in principle, be produced experimentally.

Some applications of this concept actually preceded the development of the formalism. One such application was reported by Clapp and Rifkin⁷ in a study based on molecular dynamics simulations related to a martensitic transformation. In another example of LLS calculations,

Gooding *et al.*⁸ calculated the energy along the path of a well known martensitic transformation in sodium. Work by Boyer *et al.*⁹ has focused on Si, for which a metastable phase was predicted from a systematic study of the energy associated with PALI strains. More recently, Juan and Kaxiras¹⁰ have used LLS calculations to explore structural deformations related to plastic behavior in Si under indentation.

III. THEORY OF LARGE LATTICE STRAINS

The set of all LLS which map a lattice onto itself forms an infinite group of so-called modular transformations. Such transformations are normally defined by matrices $S = BA^{-1}$ where A and B are formed from two different sets of primitive lattice vectors. For any lattice there is an infinity of choices for the primitive lattice vectors. In principle, group theory can be exploited in the analysis of functionals, such as the energy, that are invariant under

S . However, this is a difficult problem which has only been completely solved in two dimensions.^{11,12} We note that subgroups of the three dimensional modular transformations which leave a lattice plane invariant have been studied extensively in relation to twinning structures in metallurgy.¹³

The matrices S are nonsymmetric and, therefore, unphysical in the sense that the associated displacements can not be produced, even in principle, by a torque free stress. However, the same distortions can be produced by symmetric strain tensors. Following Van de Waal,⁶ we symmetrize S by multiplying it with its transpose (S^T) and taking the square root of the product, which can only be done for the diagonal matrix $S^T S$. Taking the square root of the diagonal matrix, $U^T S^T S U$ (U is the matrix of eigenvectors of S), and transforming back to the original coordinates, we get the PALI-strain transformation,

$$\tilde{S} = U[U^T S^T S U]^{\frac{1}{2}} U^T. \quad (1)$$

TABLE I. Eight types of fcc PALI-strain transformations, given by primitive vector matrices A and B together with the resultant eigenvectors ($\mathbf{e}_i, i = 1, 2, 3$) and eigenvalues ($\varepsilon_i, i = 1, 2, 3$) of the $S^T S$ matrix (the eigenvalues are given below the corresponding eigenvectors, in parentheses). \tilde{A}/A_0 is the ratio of strained to unstrained surface area and N is the number of equivalent transformations for each type.

Type	A			B			\mathbf{e}_1 (ε_1)	\mathbf{e}_2 (ε_2)	\mathbf{e}_3 (ε_3)	\tilde{A}/A_0	N
	a_1	a_2	a_3	b_1	b_2	b_3					
1	1	1	0	1	1	1	0.707	0.000	0.707	1.0404	6
	1	0	1	1	0	-1	0.000	1.000	0.000		
	0	1	1	0	1	0	-0.707	0.000	0.707		
							(2.0000)	(0.5000)	(1.0000)		
2	1	1	0	1	1	-1	0.849	0.335	0.408	1.1151	24
	1	0	1	1	0	0	-0.158	0.899	-0.408		
	0	1	1	0	1	1	-0.504	0.282	0.816		
							(3.1861)	(0.3139)	(1.0000)		
3	1	1	0	1	1	0	0.888	0.460	0.000	1.1498	12
	1	0	1	1	0	-1	-0.325	0.628	0.707		
	0	1	1	0	1	-1	-0.325	0.628	-0.707		
							(3.7321)	(0.2679)	(1.0000)		
4	1	1	1	1	1	0	-0.442	-0.576	0.688	1.1971	24
	1	0	-1	1	-1	1	0.089	0.735	0.672		
	0	1	0	0	0	1	0.893	-0.358	0.274		
							(5.5398)	(0.2565)	(0.7037)		
5	1	1	1	1	-1	0	-0.433	0.901	0.000	1.2103	12
	1	0	-1	1	0	1	0.000	0.000	1.000		
	0	1	0	0	1	-1	0.901	0.433	0.000		
							(6.7016)	(0.2984)	(0.5000)		
6	1	1	1	1	1	-1	-0.277	0.946	0.167	1.2330	24
	1	0	-1	1	-1	0	0.196	-0.115	0.974		
	0	1	0	0	0	1	0.941	0.302	-0.154		
							(3.8985)	(0.1805)	(1.4210)		
7	1	1	1	1	-1	1	-0.383	0.924	0.000	1.2761	12
	1	0	-1	1	0	-1	0.000	0.000	1.000		
	0	1	0	0	1	0	0.924	0.383	0.000		
							(5.8284)	(0.1716)	(1.0000)		
8	1	1	0	1	1	-1	0.857	0.515	0.000	1.2807	12
	1	0	1	1	-1	0	-0.365	0.606	0.707		
	0	1	1	0	0	1	-0.365	0.606	-0.707		
							(3.3508)	(0.1492)	(2.0000)		

The transformed lattice $\tilde{S}A$ is the same as $B = SA$, up to a trivial rotation $R = \tilde{S}S^{-1}$. Working with the transformed matrix \tilde{S} offers the following advantages:

(i) It provides a practical, though approximate, simplification to the functional analysis problem^{11,12} by reducing the number of shear-strain parameters from 5 to 2 (due to the symmetric nature of \tilde{S}).

(ii) It identifies orthogonal axes along which nonhydrostatic stress could be applied to achieve the desired strain, making it possible, in principle, to produce such strains experimentally.

As an example, consider a subset of \tilde{S} for the fcc lattice where the primitive lattice vectors defining the A and B matrices are confined to the shortest possible lengths. With this restriction there are eight different types of PALI-strain transformations. Representative transformations for each type are listed in Table I in increasing magnitude of distortion. They are described by the eigenvectors (\mathbf{e}_i) and corresponding eigenvalues (ε_i) of $S^T S$, with the square root of the eigenvalues giving the fractional change in distance along the directions \mathbf{e}_i . The maximum expansion (compression) directions are given by the \mathbf{e}_1 (\mathbf{e}_2) eigenvectors. A measure of the distortion is given by the ratio of the surface area \tilde{A} of a PALI-strained crystal to the area A_0 of an unstrained cubeshaped crystal with axes along the directions \mathbf{e}_i :

$$\frac{\tilde{A}}{A_0} = \frac{1}{3} [(\varepsilon_1 \varepsilon_2)^{\frac{1}{2}} + (\varepsilon_1 \varepsilon_3)^{\frac{1}{2}} + (\varepsilon_2 \varepsilon_3)^{\frac{1}{2}}]. \quad (2)$$

N is the number of equivalent transformations of a given type. For example, in type 1 transformations, the maximum compression direction (\mathbf{e}_2) can be along the (1,0,0), (0,1,0), or (0,0,1) crystallographic axes. Given one of these directions, say (0,0,1), the maximum expansion direction (\mathbf{e}_1) can be either of two directions, (1,1,0) or (1,-1,0), making a total of $N = 6$ equivalent type 1 transformations.

Next, consider the paths in strain space which result in PALI-strain transformations. Physically interesting paths are the ones that achieve the transformation with a minimum energy cost. Consequently, we define a PALI-strain path, for a given \tilde{S} , to be the path (or paths) which have the lowest maximum energy, i.e., the the lowest energy barrier. A number of issues arise concerning PALI-strain paths

(a) Most PALI-strain paths will be a sequence of other PALI transformations, presumably with smaller distortions. This is a consequence of the fact that for any given crystal a superlattice can, in principle, yield a significantly lower PALI-strain barrier (for example, treating a monatomic bcc crystal lattice as the diatomic B2 structure). If a crystal structure were treated in terms of larger and larger superlattices, successively lower PALI-strain barriers might result, owing to the increased number of relaxation parameters. Alternatively, this might lead to other distortions, such as twinning.

(b) It is likely that PALI-strain paths pass through, or near, other high symmetry structures. Some of those structures may be metastable, and may have never been identified before. By studying the energetics associated

with LLS such new structures can be identified, classified and characterized in detail.

(c) The concept of PALI strains can be effectively employed in the study of LLS in general. One aim of this paper is to indicate how this can be achieved for a prototypical covalent solid, silicon. The previous two issues also deserve further detailed exploration.

To facilitate parametrization of a PALI-strain path, we write the diagonal elements of a general strain tensor, in the coordinates which diagonalize \tilde{S} , as

$$s_{11} = (1 + f)^{-\frac{1}{3}} (1 + g)^{\frac{2}{3}}, \quad (3)$$

$$s_{22} = (1 + g)^{-\frac{1}{3}} (1 + f)^{\frac{2}{3}}, \quad (4)$$

$$s_{33} = (1 + f)^{-\frac{1}{3}} (1 + g)^{-\frac{1}{3}}. \quad (5)$$

Let $f(g)$ correspond to the direction of maximum compression (expansion). When f and g have the special values f_0 and g_0 (-0.4398 and 0.7850, respectively, for the type 2 strains in Table I), then s_{ii} are the eigenvalues of \tilde{S} . In order to determine the PALI-strain path, assuming that (f, g) are the most significant parameters, we increase f or g in small steps from (0,0) to (f_0, g_0) . At every step we keep the pair of values which produces the smallest increase of the energy, while allowing for relaxation of the remaining structural parameters. These are the off-diagonal elements of s , the volume (V) and, if the crystal structure has more than one atom per unit cell, the basis vector translation (t). This procedure may not yield identical initial and final structures in every application, except for the case of a monatomic lattice with the off-diagonal elements of s constrained to zero. However, if our procedure is applied to the various types of PALI strains in a given system, including several choices for the unit cell, then it is likely that a low energy PALI-strain path will be obtained. We demonstrate this below with the example for silicon.

IV. PHYSICALLY-ALLOWED LATTICE-INVARIANT STRAINS IN SILICON

We have used a first-principles method based on density functional theory in the local density approximation¹⁴ and atomic pseudopotentials¹⁵ (LDF for short), to calculate the energy associated with type 1 and type 2 PALI-strains in silicon. The results obtained for type 1 strains have been reported elsewhere.³ The stepping procedure described above was applied to type 2 PALI strains in silicon. This study revealed a local minimum in energy, indicating the presence of a metastable structure. The structure at the minimum, with a suitable coordinate transformation, is seen to be body centered tetragonal (space group $I4mmm$) with atoms occupying the e sites (Wyckoff notation).¹⁶ This metastable structure is described by three parameters, as shown in the inset of Fig. 1. The values of the structural parameters are $a = 6.258$ a.u., $b = 4.366$ a.u., and $c = 11.264$ a.u. Each atom is at the approximate center of a pyramid with corners occupied by the five near neighbors,

four of them almost coplanar at a distance of 4.603 a.u., and a fifth one at a distance of $b = 4.366$ a.u. We call this structure bct5, after the body centered tetragonal lattice and the fivefold coordination. The relaxed energy is 34 mRy/(unit cell) above the ground-state energy (see Fig. 1). The calculated elastic constants satisfy all the stability criteria⁹ indicating that the bct5 structure is *elastically stable*.

A different measure of stability is the frequency of long-wave optical modes: these frequencies are 520 and 340 cm^{-1} . In Fig. 1 we show the frequencies of the optical modes as they evolve during the transition from the diamond structure to the bct5 structure, obtained by our LDF calculations. The path shown here is the one defined by a physically-allowed strain connecting directly the diamond lattice to the optimized bct5 lattice. One of the modes (ω_1) becomes rather soft near the barrier configuration. However, this mode becomes again stiffer once the bct5 structure is reached, suggesting that it is stable once formed. All three optical modes should be degenerate at 0% strain and the two lower optical modes should be degenerate at 50% strain. The deviations from degeneracy are a measure of the uncertainty in our calculations,

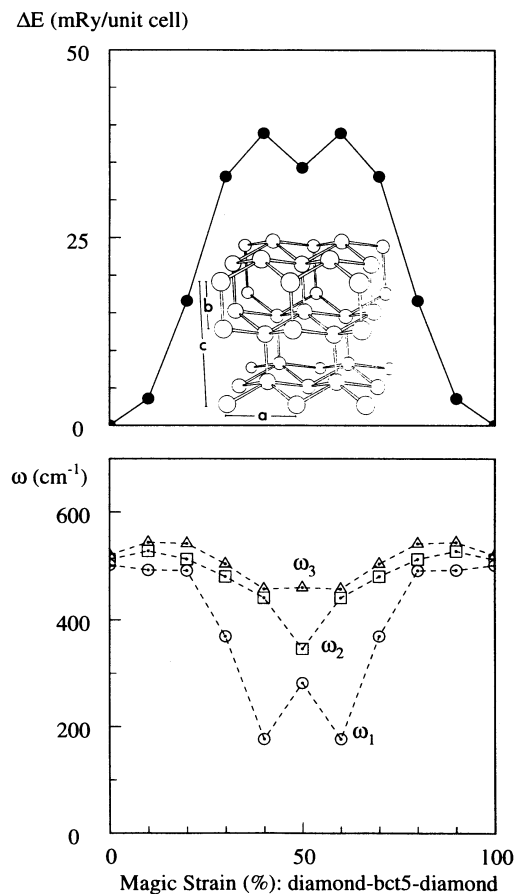


FIG. 1. Energy (upper panel) and optical mode frequencies (lower panel) during the transformation from the diamond to the bct5 phase. The physically-allowed strain path is one that leads directly from the diamond lattice to the optimal bct5 structure. The inset (upper panel) shows the bct5 structure, with the structural parameters indicated.

i.e., $\sim 50 \text{ cm}^{-1}$. A short-wave (zone boundary) instability would lower the energy without disturbing, to lowest order, the underlying lattice, aside from cell doubling along the direction of the unstable wave vector. Such distortions would further stabilize the structure against returning to the diamond lattice. This, however, requires a large change which, if it were to happen spontaneously, would point to a long-wave instability. A LDF molecular dynamics simulation might be useful to determine what temperature is needed to destabilize the bct5 structure.

The electronic properties of the bct5 phase were also studied, using our LDF approach. This phase is metallic. In Fig. 2 we show the calculated density of states (DOS) of the bct5 structure, and compare it to that of the diamond lattice (the semiconductor ground state of Si) and the high-pressure metallic phase, the β -tin lattice. In this figure, the LDF DOS was obtained from a set of 1074 independent points in the Brillouin zone of the bct lattice, and a corresponding set of equal density in reciprocal space for the other lattices. For comparison, the dashed line for the diamond lattice is from a tight-binding calculation with much denser sampling of the Brillouin zone that reproduces first-principles results and is fitted to give the correct band gap.¹⁷ The metallic character of the bct5 structure arises from the fact that the coordination of atoms (5) is higher than the valence (4). Thus, not all bonds can have covalent character. Our detailed studies of bonding in bct5 Si (Ref. 18) reveal that the four equal nearly planar bonds have metallic character, while the one shorter bond (along the c axis) is closer in nature to a covalent bond: this bond has a charge distribution very similar to that of regular covalent bonds in the diamond lattice. The β -tin structure on the other hand, has sixfold coordination, and all bonds have metallic character. Thus, we find that the bct5 structure is an intermediate phase between the

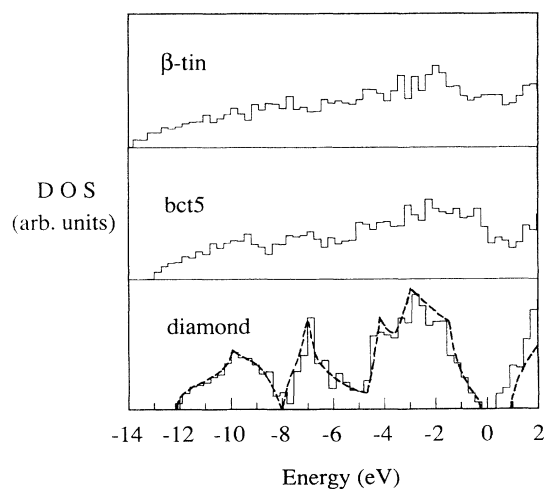


FIG. 2. Density of electronic states for three phases of Si, diamond, β tin, and bct5, obtained from LDF calculations [the dashed line is from a tight-binding calculation (Ref. 17)]. The bct5 and β -tin phases are metallic. The zero of the energy scale is the Fermi level (middle of the band gap for the semiconducting diamond crystal).

lowest-energy diamond lattice (coordination 4, semiconductor) and the high-pressure β -tin lattice (coordination 6, metal), both in terms of geometric features (bct5 has coordination 5) and in terms of electronic behavior (bct5 is metallic, but with lower DOS at the Fermi level than the β -tin phase, see Fig. 2).

V. POSSIBLE EXPERIMENTAL FORMATION OF BCT5 SILICON

A physical transformation path from the diamond lattice to the bct5 lattice can be obtained by applying the formalism of Sec. III with A corresponding to the fcc lattice and B corresponding to the bct lattice. We choose

$$A = \begin{pmatrix} 5.08 & 5.08 & 0.00 \\ 5.08 & 0.00 & 5.08 \\ 0.00 & 5.08 & 5.08 \end{pmatrix} \quad (6)$$

and

$$B = \begin{pmatrix} 6.26 & 3.13 & 0.00 \\ 0.00 & 5.63 & 0.00 \\ 0.00 & 3.13 & 6.26 \end{pmatrix} \quad (7)$$

using the lattice vectors determined by LDF calculations (in a.u.). The eigenvalues and eigenvectors of the resultant \tilde{S} matrix give the diagonal strain tensor corresponding to the physical transformation. Specifically, the requisite strain is approximately a 33% compression along the (3,14,3) direction, a 23% expansion along the (1,0,-1) direction, and a 2% expansion along the (7,-3,7) direction, in the usual (cubic) crystallographic directions.

In principle, bct5 silicon can be formed by applying a suitable uniaxial compressive stress along the (3,14,3) direction. In practice, the main difficulty will probably be the ability to control stress relief by defect formation, which results in cracking. One way around this problem is to apply the stress too quickly for such defects to form. The cracking problem might also be reduced by starting, as closely as possible, with defect free material; selecting the sample shape to be thin in the compression direction; and using small samples, to minimize defect formation. Assuming these problems can be overcome, another difficulty will be to stop the strain at the bct5 structure: If the system has too much kinetic energy associated with LLS at the top of the barrier, then the strain could pass through the bct5 structure, and onto a PALI-strained (cubic) structure. A possible procedure to overcome both these difficulties might be: to prepare first thin silicon wafers cut perpendicular to the (3,14,3) direc-

tion; then, to etch a checkerboard pattern of troughs and islands in a manner such that a 2% and 23% expansion of the islands in the (7,-3,7) and (1,0,-1) directions just fills the troughs. Contact of an island with its neighbors should stop the strain in the bct5 structure. Making the islands small ($\sim 1 \mu\text{m}$), will tend to minimize deformation due to defect mechanisms. Moreover, applying stress to the whole wafer will, in effect, carry out experiments for many samples simultaneously.

VI. SUMMARY AND CONCLUSIONS

We have discussed the implications of LLS deformations in solids and analyzed in detail the concept of PALI strains, which constitutes a useful tool for calculating such deformations. We applied that concept to the case of a prototypical covalent solid, silicon, and demonstrated how it can lead to the discovery of new metastable phases. The new phase of Si we found from application of PALI strains has interesting structural and electronic properties. The PALI-strain analysis also provides a definite prescription, through the eigenvectors of the strain matrix, of how this phase can be produced experimentally. We have discussed in detail specific methods for obtaining this phase, starting from a properly prepared sample of cubic silicon.

As a final note, we suggest that PALI-strain calculations may be very useful in developing better empirical interatomic forces for Si as well as other materials. The interatomic potentials currently used in simulations are often constructed without much consideration of LLS energetics and energy barriers. As a result, the potentials are likely to be unreliable for describing properties like the structure of the liquid state, deformations under pressure, etc. For example, the Stillinger-Weber interatomic potential for silicon¹⁹ (SW) was constructed to give reasonable properties for the liquid state. Even so, it gives approximately five near neighbors in the liquid²⁰ when in reality there are on average a little more than six.^{21,22} This discrepancy is also related to the fact that the SW potential overstabilizes the bct5 structure, which has five-fold coordination: a bct5 structure optimized with the SW potential is 14 mRy/(unit cell) higher in energy than the diamond structure. This is only 40% of the energy difference between the bct5 and diamond structures obtained by our LDF calculations. Our results on the deformations of Si that lead to the bct5 structure can be used as a guide for developing an improved form of the interatomic Si potential.

¹ J. M. Wills, O. Eriksson, P. Soderlind, and A. M. Boring, *Phys. Rev. Lett.* **68**, 2802 (1992).

² M. J. Mehl and L. L. Boyer, *Phys. Rev. B* **43**, 9498 (1991).

³ L. L. Boyer, E. Kaxiras, M. J. Mehl, J. L. Feldman, and J.Q. Broughton, in *Kinetics of Phase Transformations*, edited by M. O. Thompson, M. Aziz, and G. B. Stephenson, MRS Symposia Proceedings No. 205 (Materials Research Society, Pittsburgh, 1992), p. 477.

⁴ J. Wang, S. Yip, S. R. Phillpot, and D. Wolf, *Phys. Rev. Lett.* **71**, 4182 (1993).

⁵ L. L. Boyer, *Acta Crystallogr. Sec. A* **45**, FC29 (1989).

⁶ B. W. Van de Waal, *Acta Crystallogr. Sec. A* **46**, FC17 (1990).

⁷ P. C. Clapp and J. Rifkin, in *Phase Transformations in Solids*, edited by T. Tsakalakos, MRS Symposia Proceedings No. 21 (Materials Research Society, Pittsburgh, 1984),

- p. 643.
- ⁸ R. J. Gooding, Y. Y. Ye, C. T. Chan, K. M. Ho, and B. N. Harmon, *Phys. Rev. B* **43**, 13 626 (1991).
- ⁹ L. L. Boyer, E. Kaxiras, J. L. Feldman, J. Q. Broughton, and M. J. Mehl, *Phys. Rev. Lett.* **67**, 715 (1991); **67**, 1477 (1991).
- ¹⁰ Y.-M. Juan and E. Kaxiras, *J. Computer-Aided Materials Design* **1**, 55 (1993).
- ¹¹ I. Folkins, *J. Math. Phys.* **32**, 1965 (1991).
- ¹² A. Terras, *Harmonic Analysis on Symmetric Spaces and Applications* (Springer-Verlag, New York, 1985), Vol. I; Vol. II (1988).
- ¹³ B. A. Bilby and A. G. Croker, *Proc. R. Soc. London, Ser. A* **288**, 240 (1965).
- ¹⁴ P. Hohenberg and W. Kohn, *Phys. Rev.* **136**, B864 (1964); W. Kohn and L. J. Sham, *ibid.* **140**, A1133 (1965). The local-density approximation of D. M. Ceperly and B. J. Alder, *Phys. Rev. Lett.* **45**, 566 (1980), was used for the exchange and correlation energy.
- ¹⁵ We use norm-conserving pseudopotentials to model the atomic cores from G. B. Bachelet, D. R. Hamann, and M. Schlüter, *Phys. Rev. B* **26**, 4199 (1982). Plane waves with kinetic energy up to 16 Ry were included in the basis.
- Calculations were carried out for several uniform-density k -point meshes in order to study and establish convergence. The force exerted by one sublattice on the other was computed and used to minimize the energy with respect to relaxation of the basis.
- ¹⁶ *International Tables for X-ray Crystallography*, edited by N. F. M. Henry and K. Lonsdale (Kynoch, Birmingham, England, 1959).
- ¹⁷ D. A. Papaconstantopoulos, *Handbook of the Band Structure of Elemental Solids* (Plenum, New York, 1989), p. 234.
- ¹⁸ E. Kaxiras and L. L. Boyer, *Modeling Simulation Mater. Sci. Engineering* **1**, 91 (1992).
- ¹⁹ F. Q. H. Stillinger and T. A. Weber, *Phys. Rev. B* **31**, 5262 (1985).
- ²⁰ W. D. Luedtke and U. Landman, *Phys. Rev. B* **40**, 1164 (1989).
- ²¹ For experimental evidence see, for example, Y. Waseda, and K. Suzuki, *Z. Phys. B* **20**, 339 (1975); J. P. Gabathuler and S. Steeb, *Z. Naturforsch. A* **34**, 1314 (1979); M. Davidovic, M. Stojic, and Dj. Jovic, *J. Phys. C* **16**, 2053 (1983).
- ²² For theoretical evidence see, for example, I. Stich, R. Car, and M. Parrinello, *Phys. Rev. Lett.* **63**, 2240 (1989); *Phys. Rev. B* **44**, 4262 (1991).